Design and evaluation of liquid channel cross sections fabricated via metal fused filament fabrication

BACIKOGLU Mehmet Canberk[1,2,a *] and YAMAN Ulas[1,b]

[1]Middle East Technical University, 06800, Ankara, Turkey

[2]Radar and Electronic Warfare Systems, ASELSAN, 06830, Ankara, Turkey

[a]cbacikoglu@aselsan.com.tr, [b]uyaman@metu.edu.tr

Keywords: Metal Fused Filament Fabrication, Interior Liquid Channel, Supportless Manufacturing, Material Characterization, Quality Control

Abstract. Metal Fused Filament Fabrication is an Additive Manufacturing method of manufacturing metal parts by using filaments composed of metal powders encased in plastic binders. It is advantageous for manufacturing parts with complex geometries using a wide range of materials, including stainless steel, copper, tool steel, nickel alloys, and titanium. When support structures are not required, complex parts with interior cavities can be produced using this method. In this study, interior channel cross sections for cold plates, the main elements in cooling high-power electronic units, are designed and fabricated without the use of support structures. Specimens are made of 17-4 PH stainless steel and copper using the method with two different systems. Straight and angled interior channels are fabricated separately to investigate the characteristics of supportless manufacturing and observe the sagging or warping effects on the liquid channel faces. Surface roughness and Coordinate Measuring Machine measurements are performed for parts to check if the quality requirements are fulfilled in terms of shrinkage and assembly. Density is determined for parts using the Archimedes method and compared with the porosity results obtained from Scanning Electron Microscope.

Introduction

Additive manufacturing (AM) [1] is a method that can be used to manufacture complex parts with a novel approach. Since AM has more freedom than conventional manufacturing processes it participates more in the industry day by day. With AM, most of the limitations in traditional machining can be eliminated, pushing the limits of design, creativity, and effectiveness in manufacturing. Furthermore, rapidity and affordability are other critical properties of AM that would create an innovative path for cutting-edge technologies and products.

Polymer-based materials and metal powders constitute two major branches in AM when raw materials are considered. According to the desired material and function of the parts, several AM methods can be used. Fused Filament Fabrication (FFF) is one of the most popular AM methods that extrudes material through a nozzle and constructs a part layer by layer. On the other hand, Selective Laser Melting (SLM) [2] is a process that various type of materials in powder form are distributed over a dynamic table and melted by a high-power laser to bond metal powders to each other layer-by-layer according to the 3D geometric model of the desired part. In SLM, parts can be manufactured with aluminum alloy powders, steel powders such as maraging steel, stainless steel, etc., and titanium alloys. These materials can be selected according to the application area, i.e., structural requirements, corrosion levels, thermal properties, etc. [3].

Manufacturing parts with interior channels is challenging due to the design and production criteria. By using traditional methods such as conventional welding, brazing, and friction stir welding (FSW), structures with interior channels can be produced in a limited manner. With the help of recent advancement in AM, especially in SLM, manufacturing limitations have been

decreased. Complicated, cost-effective, and functional parts can be produced as end use artifacts [4]. Manufacturing of these parts with multi-staged conventional methods reduces freedom in design. SLM can produce structures that have voids inside due to the advantageous properties of the process itself [5]. More functional and effective parts with interior channels can be obtained with parameter optimization of AM machinery [6].

As mentioned, the SLM method is highly preferable for metal part production in AM. But a newly developed process called Metal Fused Filament Fabrication (M-FFF) is an alternative approach for metal part production. Developments and studies about this alternative show that M-FFF has great potential in metal production. For example, in the study of Henry et al. [7], 17-4 PH Stainless Steel (SS) is printed via the Atomic Diffusion Additive Manufacturing (ADAM) method on a Markforged Metal X 3D printer. It is shown that the material response is sensitive to extrusion paths and porosity is measured as 3.3% with scanning electron microscopy. Rodriguez et al. [8] manufactured parts with copper using the same 3D printer. The relative density of pure copper is found to be lower than 95%, which is worse than the other two AM technologies, SLM and Electron Beam Melting (EBM). Lower electrical conductivity, yield, and tensile strength are measured in the parts compared to the parts manufactured with SLM. Galati and Minetola characterized the same process [9]. Dimensions of the green parts and the sintered parts were evaluated. Relative density was around 90% for the sintered parts, which was far lower than the published values. Finishing operations must be performed to obtain desired surface finish and accuracy.

Design and Fabrication of Parts

Test parts are designed and manufactured using the M-FFF method to perform preliminary tests and measurements. Design and fabrication steps are explained in this section.

Design.

Parameters such as material, channel type and size, cooling path, and fin location can be optimized and adjusted to increase the thermal performance of a part used in thermal applications. Cross-section of the channel affects the thermal performance of the cold plate proportionally according to its heat transfer area. Since support structures printed inside the part cannot be removed after fabrication, interior channels must be printed without support structures to obtain the desired flow. To produce desired channel geometry, the design process must be performed according to the overhang angle criterion of the selected material.

Copper is used for manufacturing with the M-FFF method, which has advantageous thermal properties for thermal applications. Since pure copper's overhang angle requirement is 50º, angles larger than 50º are chosen for supportless manufacturing of channels. As stated before, the thermal performance of different types of channel cross-sections is one of the key points. Four different channel cross-sections are designed to control the quality of the test parts. 50º of overhang angle is considered during the design of these cross sections. In the first cross-section, droplet alike cross section (CS1) is designed, which is a typical shape for supportless manufacturing. A bigger flow area is formed in the second cross-section (CS2), which is like a triangle. In the third one, a column is constituted in the middle of the cross-section (CS3) to increase the heat transfer area. In the fourth cross section (CS4), two fin structures are added throughout the channel path. Essential dimensions of cross sections are remarked in Fig. 1. Specified cross sections have different perimeters of 12.9 mm, 15.7 mm, 20.7 mm, and 23.2 mm, respectively, which will directly affect the heat transfer area of the interior channel.

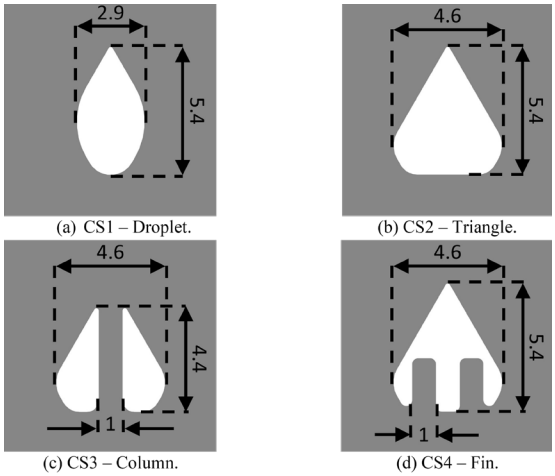

Fig. 1. Dimensions of the cross sections in mm.

Two kinds of testing parts are designed to observe the manufacturability of the cross-sections. In the first testing part (Fig. 2a), the aim is to monitor the quality of the cross-section, supportless manufacturing results, and uniformity of sintered part over a straight channel. In the second part, the same parameters are utilized for the angled channels in Fig. 2b. Also, a cylinder part is designed with 10 mm in diameter and 10 mm in height to determine the density and porosity parameters of copper.

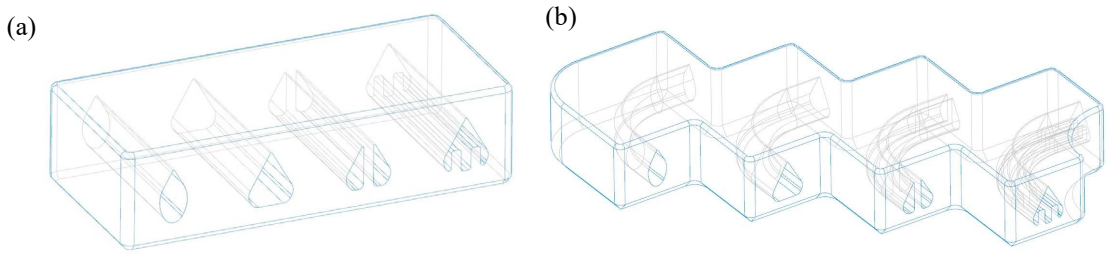

Fig. 2. Wire frames of the straight and angled test parts: (a) straight channels, (b) angled channels.

Outer regions of the parts don't include sharp corners like channel cross sections. Radii are created to eliminate sharp corners and residual stress that shows up during sintering, and to conserve the part's uniformity. In the M-FFF systems, the desired part is manufactured larger than the desired part considering shrinkage due to binder material in filaments. Printing simulation of straight and angled test parts made of copper are demonstrated in Fig. 3. Part details related to printing are noted in Table 1.

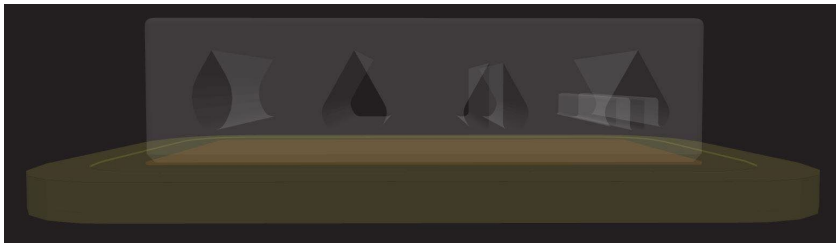

Fig. 3. Support control and layer view in the CAM software. Yellow is raft, orange is ceramic release and white is the part.

Table 1. Properties of the test parts as stated in the CAM software of the M-FFF system.

Test parts	*Straight*	*Angled*	*Cylinder*
Printed dimensions [mm]	46.4x20.9x11.9	66.2x66.2x11.9	Ø11.6x11.9
Final part dimensions [mm]	40x18x10	57x57x10	Ø10x10
Print time [hour]	7.2	13.2	2.5
Wash time [hour]	12.5	31	20
Dry time [hour]	4	4	4
Printed part mass [g]	89.6	178.2	16.3
Final part mass [g]	53.7	111	6.5
Number of wall layers	4	4	4

Fabrication.

Straight and angled interior channels are fabricated separately to investigate the characteristics of supportless manufacturing and observe the pouring or warping effects on the liquid channel faces. The fabrication process is performed using The Metal X 3D printer of Markforged. The Metal X Printer uses the ADAM method, which has a build volume of 300x220x180 mm. The printer has two nozzles, for metal material extrusion and ceramic support release material extrusion. The Metal X printer has two resolution options, 50 and 200 μm. After printing desired parts, green parts, which include both plastic and metal materials inside, are acquired Fig. 4. Green parts are subjected to a washing process to remove binders and clean parts, which results in obtaining brown parts. Then the sintering process is employed on brown parts to remove all plastic and binder materials and bond metal powders together. To obtain uniform shrinkage and prevent warping during sintering, the part is printed on a raft material, the same material as the desired part. A thin layer of ceramic powder between the green part and the raft helps to separate the parts.

Fig. 4. Green state of the manufactured straight and angled test parts.

While printing the test parts, 200 μm resolution is used. Test parts are made of 17-4 PH SS and copper. Since only 17-4 PH SS was initially available in producing company, a straight test part is manufactured with 17-4 PH SS (Fig. 5) to control the convenience of support generation on the CAM software. Then, the straight and angled (Fig. 6) test parts are produced with copper. Also, the cylinder part used in some characterization tests is shown in Fig. 7.

Fig. 5. Straight test part made of 17-4 PH SS.

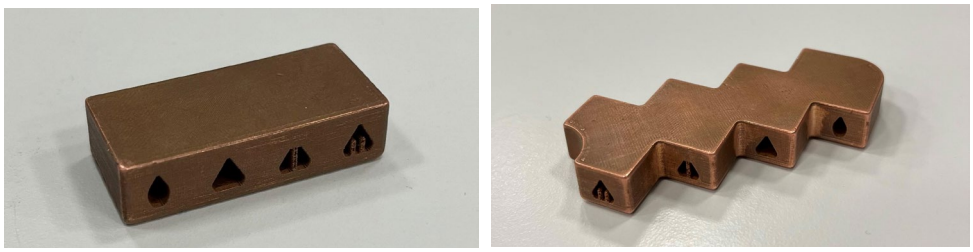

Fig. 6. Straight and angled test parts made of copper.

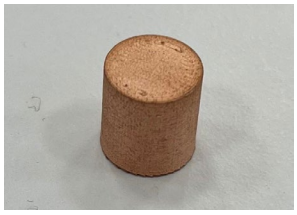

Fig. 7. Cylinder test part made of copper.

Material Characterization and Quality Control

Before material characterization and quality control tests, the test parts are inspected visually. High surface roughness at the bottom face of the test parts is observed due to the ceramic layer between the raft and the metal part. Some defects on the column structure of CS3 and the fin structure of CS4 are observed. Interior faces of the straight and angled test parts are less rougher than the internal faces of the channels manufactured with the SLM method. Measured masses of the test parts and the mass values calculated in the CAD software are stated in Table 2.

Coordinate Measuring Machine (CMM).

Dimensions of the straight and the angled test parts are measured with the Delta Slant gantry type CMM. Mainly, outer dimensions of the test parts are measured with the CMM, such as width, length, and height. For CS1 and CS2, channel height and width are measured with CMM as appropriately as possible. For CS3 and CS4, the CMM probe couldn't touch the faces of the interior channel since the probe diameter is 0.8 mm and the probe is bent while touching the interior faces. In addition, because of the deterioration of the column and the fin structures of CS3 and CS4, the risk of breaking the probe is increased. Thus, a microscope and a digital caliper are used for the measurement of these dimensions.

Table 2. Masses of the test parts.

Test part	Material	Mass in CAD [g]	Actual mass [g]	Difference
Straight	17-4 PH SS	48.9	43.0	-12.1%
Straight	Copper	53.7	54.3	+1.1%
Angled	Copper	111	112.8	+1.6%
Cylinder	Copper	6.5	6.7	+3.1%

Outer dimensions of the test parts are shown in Table 3. When the results are elaborated, it is seen that 17-4 PH SS part has more deviation than the copper counterparts in x- and y-axis, which are length and width, respectively. But in z-axis, 17-4 PH SS has a better result. Similar deviations are observed when the outer dimensions of the copper test parts are compared. For all outer dimensions in all axes of the three test parts, actual dimensions are greater than the CAD models, and much higher tolerances are obtained than the traditional manufacturing methods.

Table 3. Outer dimensions of the test parts.

	Part	*Straight*	*Straight*	*Angled*
	Material	17-4 PH SS	Copper	Copper
Width [mm]	**CAD dimension**	18	18	57
	Actual dimension	18.43	18.14	57.16
	Deviation	0.43	0.14	0.16
Length [mm]	**CAD dimension**	40	40	57
	Actual dimension	40.57	40.27	57.11
	Deviation	0.57	0.27	0.11
Height [mm]	**CAD dimension**	10	10	10
	Actual dimension	10.09	10.29	10.24
	Deviation	0.09	0.29	0.24

The results of the essential dimensions of channel cross-sections are shown in Table 4. Similar results are obtained when the straight and the angled copper test parts are compared. Dimensions for the channel height are less than the nominal dimensions. Fin thicknesses are mostly greater than the nominal dimensions, but there are some deteriorations in the fin thicknesses of both structures. These deteriorations affected average fin thickness negatively. 0.82 mm and 1.32 mm of fin thicknesses are observed when the lower and the upper limits are considered, which can be originated from spoilt extrusion, pouring, and uncontrolled shrinkage, as seen in Fig. 8.

CMM measurements of the cylinder test parts are shown in Table 5. The height of the cylinder is measured to be more than the nominal dimension. The actual diameter of the cylinder is 9.9 mm, with a 0.1 mm deviation from the designed value, which is acceptable when compared with the traditional machining methods.

Surface roughness.

Surface roughness is a surface property that determines the surface quality of a part. Summation of deviations in the normal vector of surface expresses surface roughness. Surface roughness affects the appropriateness of assembly, friction, and wear on the surface. Ra value indicates an arithmetic average of height deviation from the mean profile of the surface, and Rz value indicates the distance between the upper and lower points on the surface that is investigated. Surface roughness of the test parts is measured by the Mitutoyo Surftest SJ-400 device. Ra and Rz values are measured for upper surface, side surface, and bottom surface of the test parts and are indicated in Table 6.

Table 4. Dimensions of the channel cross sections.

	Part	*Straight*	*Angled*
	Material	Copper	Copper
CS1 Height [mm]	**CAD dimension**	5.5	5.5
	Actual dimension	5.34	5.35
	Deviation	-0.16	-0.15
CS2 Height [mm]	**CAD dimension**	5.5	5.5
	Actual dimension	5.36	5.33
	Deviation	-0.14	-0.17
CS3 Height [mm]	**CAD dimension**	4.63	4.63
	Actual dimension	4.18	4.11
	Deviation	-0.45	-0.52
CS3 Fin Thickness [mm]	**CAD dimension**	1.0	1.0
	Actual dimension	1.25	1.07
	Deviation	0.25	0.07
CS4 Height [mm]	**CAD dimension**	5.5	5.5
	Actual dimension	5.36	5.37
	Deviation	-0.14	-0.13
CS4 Fin Thickness [mm]	**CAD dimension**	1.0	1.0
	Actual dimension	0.99	1.05
	Deviation	-0.01	0.05

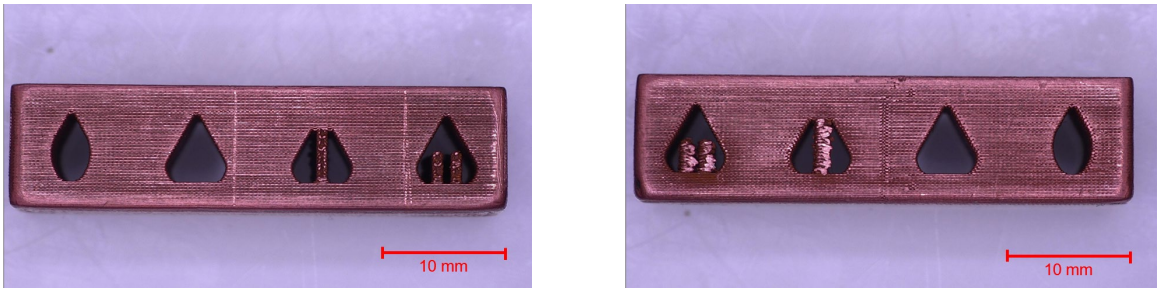

a) front view b) back view

Fig. 8. Deteriorations on the fin structures of CS3 and CS4 of the straight test parts.

Table 5. Dimensions of the cylinder test part.

	Part	*Cylinder*
	Material	Copper
Diameter [mm]	**CAD dimension**	10.0
	Actual dimension	9.9
	Deviation	-0.1
Height [mm]	**CAD dimension**	10.0
	Actual dimension	10.34
	Deviation	0.34

Table 6. Surface roughness of the test parts.

		Top Surface		Side Surface		Bottom Surface	
Part	**Material**	**Ra [µm]**	**Rz [µm]**	**Ra [µm]**	**Rz [µm]**	**Ra [µm]**	**Rz [µm]**
Straight	Copper	1.95	12.01	6.07	31.65	26.02	105.3
Angled	Copper	1.33	8.3	12.33	51.5	32.79	129.2

As seen from Ra and Rz values of the straight and the angled copper test parts, results are similar to each other. When surfaces are compared, the best surface quality is obtained on the upper surface, which is close to the surface roughness values of machined parts. Regarding the side surface, Ra and Rz values are fairly average and increased compared to the upper surface since the staircase effect is more perceivable. But on the bottom surface, surface roughness is increased significantly due to the ceramic layer residuals. Due to the sintering of the part, ceramic layer becomes more powdery and spoils the quality of the bottom surface of the final part.

Archimedes method.

Undesired porosity throughout the parts decreases the strength of the material and can cause crack propagation after force is applied. Also, density must be specified for the unknown materials to calculate other material properties and obtain the mass. To gain insight into the porosity and density of parts, Archimedes method, a measurement procedure to determine the density of parts, is applied for copper cylinder test parts. This method is based on measuring the test part's weight in air and water where the part is fully submerged. This difference gives the buoyancy force, which equals the weight of the displaced fluid. Since the part is completely submerged and the volume is the same for both cases, the ratio of the density of the test part and the density of the fluid equals to the ratio of the weight of the test part and the weight of the displaced fluid. As built parts are used, which means no machining or grinding operation is applied on the cylinder specimens. Density is evaluated according to the ISO 3369 test standard. Archimedes method is performed by using Precis XB 220A device at 24ºC ambient temperature. Measured densities of copper specimens are calculated via Eq. 1; where m_a is the mass of test piece determined by weighing in air, m_w is the mass of test part in liquid, and ρ_w is the density of distilled water at 24ºC ambient temperature which equals to 0.9973 g/cm^3 as specified in the standard. After the specimens are laid on the attachment in the water side of the device, no significant air bubbles are observed on the outer surfaces of them.

$$\rho = \left(\frac{m_a}{m_a - m_w}\right)\rho_w \quad (1)$$

After measuring the masses of the test parts in air and water, respectively, density values are obtained. The average density value for the test parts is found as 8.6462 g/cm3 where the standard deviation is 0.0383. Relative density is calculated as 96.50%, where Markforged specifies it as 98% in the datasheet for copper used on the 3D printer. That means copper specimens have 3.50% porosity inside on average. Defects in the part, such as open pores or closed pores infilled with air or bubbles, can be the main reason for the difference in relative density, which increases the porosity level of the parts.

Scanning Electron Microscope (SEM) Analysis.

SEM is used to analyze the porosity of the copper parts after sectioning. Manufactured copper cylinder parts are used for sectioning; specimens are machined by a lathe and ground with 800-grit sandpaper to obtain a surface as smooth as possible. Then, the Phenom XL G2 SEM is used to observe sections of the parts in a detailed manner. Randomly distributed voids are detected during screening. Although grinding marks are observed, porous structures are obtained as separable throughout the section. There is no significant distribution of voids on the sectioned

surface according to the occurrence in some specific areas, such as around the peripheral or close to the center. Screening images show that voids are distributed randomly around the sectioned surface. Some images obtained with the SEM are demonstrated in Fig. 9. Images are subjected to image processing on ImageJ software to perform porosity analysis. 3.92% of porosity is obtained, close to the result obtained in the Archimedes method. Average area of the pores is 18.08 μm^2, which corresponds to an average diameter of 4.8 μm.

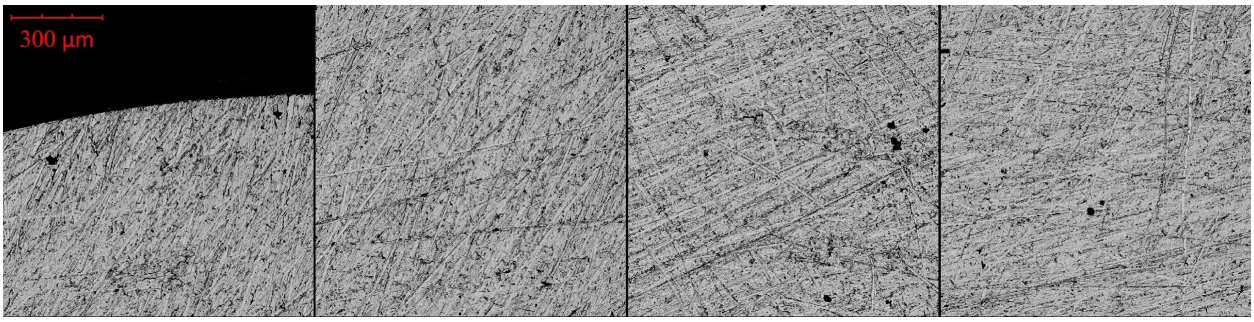

Fig. 9. Some SEM images of the cylinder test parts.

X-Ray Scanning.

X-ray imaging is performed to investigate the interior quality of the channel sections by taking images of the parts. X-ray inspection is done by using the Nordson Dage Quadra 7 instrument with an X-ray power of 160 kV. Details of the channel sections are illustrated in Fig. 10. Since the test parts subjected to X-ray scans are made of copper, details of the channel sections are obtained coarsely in observation because of the high density of copper. As a result of changing the areas of the cross sections, a blurry view around the channel occurs. The column structure of CS3 and the fin structure of CS4 is observed more precisely due to the constant and straight sections.

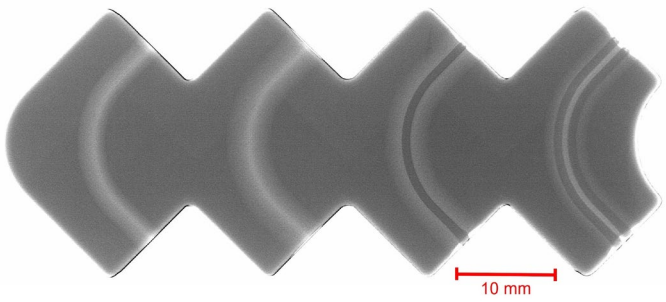

Fig. 10. X-ray inspection of the angled test part.

Summary

In this study, manufactured test parts using the M-FFF method are subjected to preliminary material characterization and quality control tests such as measurement of *surface roughness*, determination of dimensional accuracy with the *CMM*, scanning of parts with the *X-ray* device, calculation of the density with the *Archimedes method* and determination of porosity within the part with the *SEM analysis*. According to the CMM results, dimensions of the test parts are mostly greater than the nominal dimensions. For overall dimensions of the channel sections, mostly smaller dimensions are measured. Surface roughness results are significantly satisfying for upper and side surfaces compared to the SLM method. Thus, the M-FFF method can be used for the parts

that include liquid paths in terms of pressure drop. The result of X-ray scan shows that a device with more powerful X-ray source must be used to obtain images with finer details. Obtained results of density and porosity are lower than the datasheet results, which means that the manufactured parts must be qualified in terms of strength and leakage according to the application area. Despite these, the M-FFF method can be used for fast prototyping due to its speed, price, and modularity. As future works, process parameters and product range may be improved for the M-FFF method.

Acknowledgement
This work was supported in part by Middle East Technical University under the project contract ADEP-302-2022-11183.

References

[1] W.E. Frazier, Metal additive manufacturing: a review, J. Mater. Eng. Perform. 23 (2014) 1917-1928. https://doi.org/10.1007/s11665-014-0958-z
[2] W.J. Sames, F.A. List, S. Pannala, R.R. Dehoff, S.S. Babu, The metallurgy and processing science of metal additive manufacturing, Int. Mater. Rev. 61 (2016) 315-360. https://doi.org/10.1080/09506608.2015.1116649
[3] J. Armen, H.A. Bruck, Improving contact resistance in metal–ceramic heat exchangers running liquid metal by additive manufacturing and ceramic tubes with electroplated films, Int. J. Adv. Manuf. Technol. 113 (2021) 2101-2119. https://doi.org/10.1007/s00170-021-06813-0
[4] R.P.P. da Silva, M. V. V. Mortean, K.V. de Paiva, L.E. Beckedorff, J.L.G. Oliveira, F.G. Brandão, A.S. Monteiro, C.S. Carvalho, H.R. Oliveira, D.G. Borges, V.L. Chastinet, Thermal and hydrodynamic analysis of a compact heat exchanger produced by additive manufacturing, Appl. Therm. Eng. 193 (2021) 116973. https://doi.org/10.1016/j.applthermaleng.2021.116973
[5] Z. Gobetz, A. Rowen, C. Dickman, K. Meinert, R. Martukanitz, Utilization of Additive Manufacturing for Aerospace Heat Exchangers, Pennsylvania State University State College United States, (2016).
[6] D. Bacellar, V. Aute, Z. Huang, R. Radermacher, Design optimization and validation of high-performance heat exchangers using approximation assisted optimization and additive manufacturing, Sci. Technol. Built Environm. 23 (2017) 896-911. https://doi.org/10.1080/23744731.2017.1333877
[7] T.C. Henry, M.A. Morales, D.P. Cole, C.M. Shumeyko, J. C. Riddick, Mechanical behavior of 17-4 PH stainless steel processed by atomic diffusion additive manufacturing, Int. J. Adv. Manuf. Technol. 114 (2021) 2103–2114. https://doi.org/10.1007/s00170-021-06785-1
[8] J. Rodriguez, J.I. Vicente, J.C. Ezeiza, A. Zuriarrain, P.J. Arrazola, X. Badiola, E. Dominguez, D. Soler, Mechanical and electrical properties of additively manufactured copper. In IOP Conference Series: Mater. Sci. Eng. 1193 (2021) 012034. https://doi.org/10.1088/1757-899X/1193/1/012034
[9] M. Galati, P. Minetola, Analysis of density, roughness, and accuracy of the atomic diffusion additive manufacturing (ADAM) process for metal parts, Materials 12 (2019) 4122. https://doi.org/10.3390/ma12244122